



ELSEVIER

Available online at www.sciencedirect.com

SCIENCE @ DIRECT®

Nuclear Instruments and Methods in Physics Research B 210 (2003) 266–271

NIM B
Beam Interactions
with Materials & Atomswww.elsevier.com/locate/nimb

Proton beam writing of passive waveguides in PMMA

T.C. Sum^{*}, A.A. Bettiol, H.L. Seng, I. Rajta¹, J.A. van Kan, F. Watt*Department of Physics, Blk S12, Faculty of Science, Research Centre for Nuclear Microscopy, National University of Singapore,
2 Science Drive 3, Singapore 117542, Singapore*

Abstract

Symmetric y-branch buried channel waveguides in *poly-methylmethacrylate* (PMMA) were fabricated by *proton beam writing* using a focused sub-micron beam of 1.5 and 2.0 MeV protons with a dose ranging from 25 to 160 nC/mm² (i.e. $\sim 1.6 \times 10^{13}$ to 1.0×10^{14} particles/cm²) and beam currents of approximately 5–10 pA. The proton beam modifies the PMMA (i.e. changes the refractive index), forming buried channel waveguides near the end of range. The buried channel waveguides were end-coupled with monochromatic light (633 nm) and the transmitted intensity profiles were measured, indicating an intensity distribution of 0.45/0.55 from each branch. The surface compaction of the PMMA as a result of the irradiation for doses up to 160 nC/mm² was also investigated. From these investigations, the optimal fabrication conditions for proton beam writing of PMMA were established. Waveguides of arbitrary design can be easily fabricated using proton beam writing, making the technique ideal for the rapid prototyping of optical circuits.

© 2003 Elsevier B.V. All rights reserved.

PACS: 07.78.+s; 42.70.Jk; 42.82.Cr; 42.82.Et

Keywords: Proton beam writing; Buried channel waveguides; PMMA; Surface compaction

1. Introduction

Polymers are an interesting class of materials with many unique characteristics such as their high optical clarity, low attenuation, and their excellent weathering ability. Today, literally hundreds of polymeric materials have found widespread use in the manufacture of microwave, electronic and photonic systems [1]. This use is attributed to the ease of processing and fabrication of polymers.

Their structures can be easily tailored to provide a wide range of physical properties.

In contrast to inorganic materials such as LiNbO₃ and InP, polymeric optical waveguides offer a cost-effective solution for many telecommunication applications. Some common techniques used for polymeric waveguide fabrication include ion implantation [2,3], photolithography and reactive ion etching [4,5] and photobleaching [6,7]. However, these latter methods involve numerous processing steps and require long fabrication times. One of the biggest advantages of ion implantation over the latter techniques is that the waveguides can be easily fabricated at a controllable depth by simply selecting the incident ion energy, since the ions have a well-defined path and range in polymers.

^{*} Corresponding author. Tel.: +65-6874-4953; fax: +65-6777-6126.

E-mail address: scip1089@nus.edu.sg (T.C. Sum).

¹ Present address: Institute of Nuclear Research of the Hungarian Academy of Sciences, Hungary.

The use of high-energy (MeV) ion implantation to fabricate polymer waveguides has been reported by Ruck et al. and Hong et al. Ruck et al. fabricated buried channel waveguides in poly-methyl-methacrylate (PMMA) by irradiating PMMA through a Si mask as well as by direct masking of the PMMA substrate using a Ni shim, while Hong et al. fabricated planar waveguides in PMMA using ion implantation [8,9]. Direct-writing with a focused MeV proton beam to fabricate linear buried channel waveguides in fused silica have been reported by Roberts and von Bibra [10] and von Bibra et al. [11]. The advantage of using a direct-write focused ion beam of high-energy (MeV) light ions (e.g. H^+) is that buried channel waveguides can be fabricated without the need of a mask.

In this paper, we report on the application of proton beam writing to fabricate symmetric y-branch buried channel waveguides in PMMA. Proton beam writing uses a focused sub-micron beam of high-energy protons to direct-write on a suitable material, such as polymers, fused silica,

quartz, sapphire, etc. Unlike proton beam micromachining [12–14], proton beam writing of polymers does not involve any chemical development processes after the irradiation.

Proton beam writing can be used to fabricate any arbitrary waveguide pattern (e.g. the Mach-Zehnder interferometer, directional couplers etc.). A symmetric y-branch design as shown in Fig. 1(a) was chosen to demonstrate the light guidance in the two branches. Sub-micron beam resolution is extremely critical for proton beam writing as it is important to direct-write the optical pathways accurately in order to realize the optimal design and to minimize optical losses. For the case of a symmetric y-branch, this is crucial for the cosine S-bend segment near the intersection with the linear taper segment.

One other objective of this study is to optimize the conditions to fabricate waveguides in PMMA using a focused proton beam. Unlike fused silica, the damage threshold of PMMA is much lower. It is important to find out the optimum irradiation

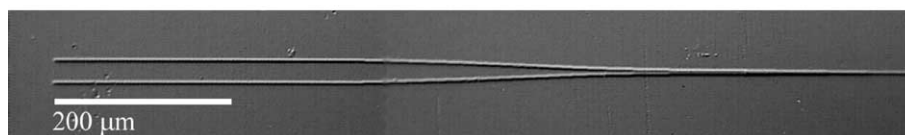
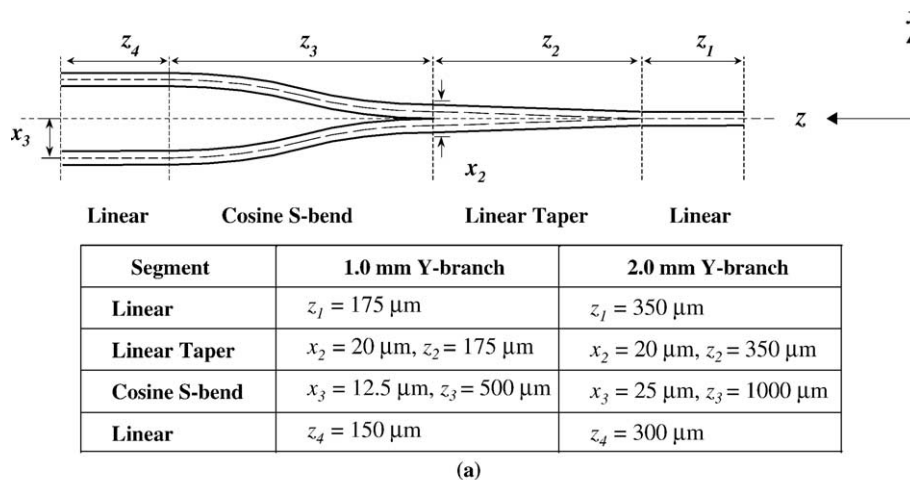


Fig. 1. (a) Schematic of the y-branch waveguide design used in the fabrication. Both 1.0 and 2.0 mm waveguides were fabricated. (b) Differential interference contrast (DIC) image of a y-branch waveguide of length 1.0 mm fabricated using 1.5 MeV protons and a dose of 75 nC/mm^2 (i.e. $\sim 4.7 \times 10^{13}$ ions/cm²).

parameters such as the proton dose, beam energies and beam currents to avoid adverse damage to the PMMA (i.e. blistering of the surface, bubble formation at the end of range, etc.) [15].

As in the case for any direct-write technique compared with masked lithography, the manufacturing throughput from proton beam writing is expected to be low. Nonetheless, proton beam writing offers us great flexibility to fabricate waveguides of arbitrary patterns and this is an asset for the rapid prototyping of optical circuits.

2. Experimental

Optical waveguides require lateral confinement; therefore the ion beam modification must be carried out with lithographic definitions of the optical pathways. In proton beam writing, the incident beam modifies the PMMA (i.e. changes the refractive index) along these optical pathways, forming the buried channel waveguides. Proton beam writing is carried out using proton beams from the *High Voltage Engineering Europa 3.5 MeV Singletron*TM accelerator [16] at the Research Centre for Nuclear Microscopy, Department of Physics, National University of Singapore. PMMA sheets from *Röhm (Plexiglas® GS233)* with a thickness of 2.0 mm were used in the fabrication of these buried channel waveguides. Typically, the samples were cut to a size of 1.5 cm × 0.5 cm.

Y-branch waveguides of width 10 μm with a length of 1.0 and 2.0 mm were fabricated by magnetically scanning the proton beam over the PMMA. A description of the scanning system and the RBS dose normalization procedure can be found in [17]. The fabrication was carried out using both 1.5 and 2.0 MeV protons with a sub-micron beam spot. The range of these protons in the PMMA is approximately 39 and 62 μm, respectively. The doses used in the fabrication ranges from 25 to 160 nC/mm² (i.e. $\sim 1.6 \times 10^{13}$ to 1.0×10^{14} particles/cm²). The beam currents were kept to a low value of 5–10 pA as preliminary results have shown that the surface of the PMMA surface blisters and trapped gases near the end of range are formed when higher currents were used.

After the irradiations, the samples were edge-polished until the end-faces of the waveguides were exposed with a remaining roughness of less than 60 nm. The waveguides were then end-coupled with monochromatic light (633 nm) using a single mode optical fiber (*3M single mode fiber FS-SN-3224*, core ~ 4 μm). Index matching oil from *Nye Optical Products (NCF-446, n = 1.46)* was applied between the waveguide end-faces and the optical fiber to minimize the light scattering from the PMMA surface. The output light was imaged with a CCD camera mounted on a microscope with a 20× long working distance microscope objective lens (NA = 0.3). The images were obtained in an 8-bit mode (i.e. a resolution of 256 gray levels).

The atomic force microscope (AFM) is an excellent instrument to assess the surface modification to the PMMA after the irradiation (e.g. surface damage, uniformity of the irradiation, surface compaction etc.). The irradiated pathways were profiled using tapping mode AFM (*Digital Instruments Dimension*TM 3000 SPM) over an area of 82 × 82 μm² centred on the two branches, with the branches aligned parallel to the slow scan axis.

3. Results and discussions

Fig. 1(b) shows the top view of a 1.0 mm long y-branch buried channel waveguide. The energy deposition due to the passage of ions through a polymer is mainly due to electronic stopping. Based on the above energy and dose range, PMMA undergoes chain scission [18]. The changes in the chemical and physical structure of the polymer lead to the compaction and densification of the remaining material, thus increasing the refractive index. The largest change of refractive index occurs near the end of range where the maximum amount of energy is deposited. With this high refractive index layer (the core) surrounded by a lower refractive index cladding (the unmodified PMMA), light guidance is possible. A cross-sectional view of the polished end-face of a waveguide of length 2.0 mm is shown in Fig. 2.

Fig. 3(a) shows an image of an illuminated y-branch buried channel waveguide. The waveguide core is estimated to be approximately 10 μm

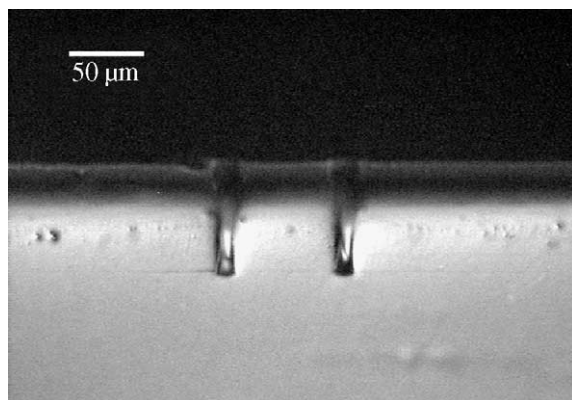
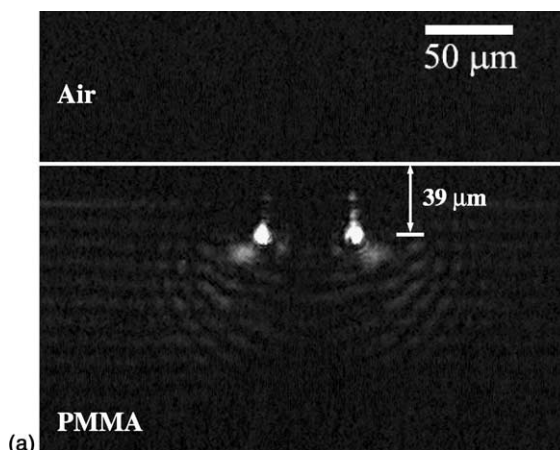


Fig. 2. DIC image of the cross-section of a y-branch waveguide of length 2.0 mm fabricated with 1.5 MeV protons and a dose of 75 nC/mm^2 (i.e. $\sim 4.7 \times 10^{13}$ ions/cm 2).

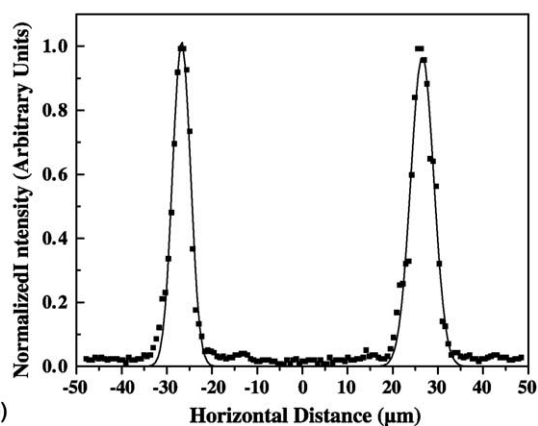
across laterally and vertically. It is located at a distance of $39 \mu\text{m}$ below the PMMA surface, in agreement with TRIM simulations. Interference fringes, which are faintly visible, are caused by the internal reflections from the surface of the PMMA substrate due to the scattering of the laser light into the cladding. The normalized intensity distributions of the two branches shown in Fig. 3(a) are given in Fig. 3(b). The intensity distribution for each branch was fitted using a gaussian fit as indicated by the solid lines. By integrating the area under each gaussian, the ratio of the distributions from each branch was found to be 0.45/0.55.

Fig. 4 shows an $82 \times 82 \mu\text{m}^2$ AFM surface scan over the surface of a buried y-branch waveguide. The AFM images were flattened using a low order polynomial fit. Such manipulation of raw AFM data is usually performed to remove the image artefacts (i.e. vertical offsets between scan lines), which may be caused by vertical (Z) scanner drift, image bow or any non-linear behaviour in the piezo scanning mechanism.

Fig. 5 shows the measured surface compaction of the waveguides as a function of dose for both 1.5 and 2.0 MeV protons. The data for each series was fitted by a least squares fit and the uncertainty in the measured values were estimated from the standard deviation of the surface roughness and the differences in the processed images as a result of the flattening process. The amount of compac-



(a)



(b)

Fig. 3. (a) 633 nm light emitted from the branches of a 2.0 mm long y-branch waveguide. The waveguide was fabricated with 1.5 MeV protons and a dose of 75 nC/mm^2 (i.e. $\sim 4.7 \times 10^{13}$ ions/cm 2). (b) Normalized intensity distribution of the emitted light of y-branch shown in (a). The solid lines represent the gaussian fits for these distributions.

tion of the polymer surface increases as the dose increases. From these results, it can be seen that the degree of compaction for the two different energies are rather similar. For an incident beam of 1.5 and 2.0 MeV protons and a dose of 100 nC/mm^2 (i.e. $\sim 0.63 \times 10^{14}$ particles/cm 2), the compacted depth of the PMMA is measured to be approximately 140 nm. This compaction value is very small compared to the range of 1.5 and 2.0 MeV protons in PMMA (i.e. 39 and 62 μm respectively). Hence, based on the current dose, the surface shrinkage of PMMA due to modification would

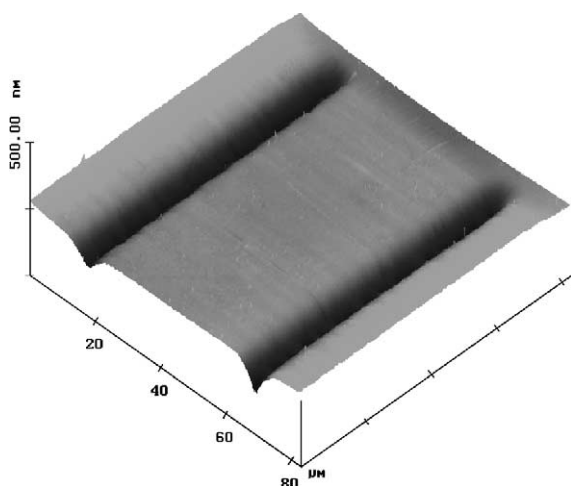


Fig. 4. AFM image of the surface of a 10 μm wide y-branch waveguide fabricated using 1.5 MeV protons and a dose of 75 nC/mm^2 (i.e. $\sim 4.7 \times 10^{13}$ ions/ cm^2).

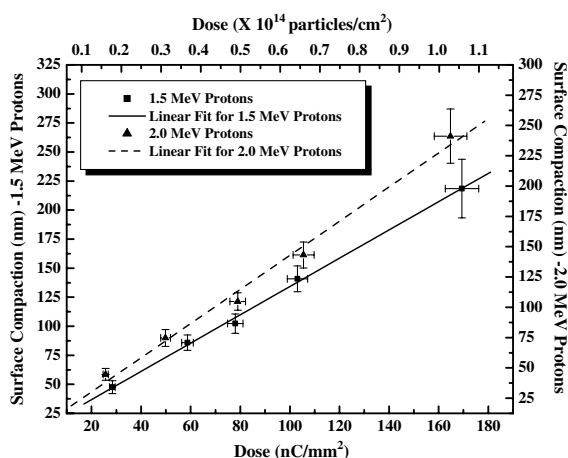


Fig. 5. Graph of surface compaction of PMMA as a function of the incident proton dose and proton energies.

have negligible effect on the accuracy of the depth at which the buried channel waveguides are fabricated.

4. Conclusions

We have demonstrated the feasibility to fabricate buried channel waveguides in PMMA by

proton beam writing. The waveguides were successfully fiber-coupled and the intensity profiles were measured. Further work on characterizing these buried channel waveguides (such as obtaining the refractive index profile, the measurement of the propagation losses etc.) is currently in progress. For the range of doses used to fabricate the y-branch waveguides, the surface compaction of the PMMA as a consequence of the modification was found to be minimal and would have negligible effect on the depth control. Proton beam writing offers us great versatility for waveguide fabrication, and it is ideal for the rapid prototyping of optical circuits.

Acknowledgements

A Defence Innovative Research Programme (DIRP) grant from the Defence Science and Technology Agency (DSTA), Singapore, supported this work.

References

- [1] W.F.X. Frank, A. Schösser, A. Stelmaszyk, J. Schulz, in: R.A. Lessard, W.F.X. Frank (Eds.), *Polymers in Optics, Physics, Chemistry and Applications*, SPIE Optical Engineering Press, 1996, p. 65.
- [2] W.F.X. Frank, J. Kulisch, H. Franke, D.M. Ruck, S. Brunner, R.A. Lessard, SPIE 1559 (1991) 344.
- [3] W.F.X. Frank, A. Schösser, S. Brunner, F. Linke, T.K. Stempel, M. Eich, SPIE 1774 (1992) 268.
- [4] M. Hikita, Y. Shuto, M. Amano, R. Yoshimura, S. Tomaru, H. Kozawaguchi, *Appl. Phys. Lett.* 63 (1993) 1161.
- [5] W. Wang, D. Chen, H.R. Fetterman, Y. Shi, W.H. Steier, L.R. Dalton, *Appl. Phys. Lett.* 65 (1994) 929.
- [6] M.B.J. Diemeer, F.M.M. Suyten, E.S. Trommel, A. McDonach, J.M. Copeland, L.W. Jenneskens, W.H.G. Horsthuis, *Electron. Lett.* 26 (1990) 379.
- [7] Y. Shi, W.H. Steier, L. Yu, M. Chen, L.R. Dalton, *Appl. Phys. Lett.* 58 (1991) 1131.
- [8] D.M. Ruck, S. Brunner, K. Tinschert, W.F.X. Frank, *Nucl. Instr. and Meth. B* 106 (1995) 447.
- [9] W. Hong, H.J. Woo, H.W. Choi, Y.S. Kim, G.D. Kim, *Appl. Surf. Sci.* 169–170 (2001) 428.
- [10] A. Roberts, M.L. von Bibra, *J. Lightwave Technol.* 14 (11) (1996) 2554.
- [11] M.L. von Bibra, A. Roberts, S.D. Dods, *Nucl. Instr. and Meth. B* 168 (2000) 47.

- [12] J.A. van Kan, J.L. Sanchez, B. Xu, T. Osipowicz, F. Watt, Nucl. Instr. and Meth. B 148 (1999) 1085.
- [13] T. Osipowicz, J.A. van Kan, T.C. Sum, J.L. Sanchez, F. Watt, Nucl. Instr. and Meth. B 161–163 (2000) 83.
- [14] J.A. van Kan, A.A. Bettioli, B.S. Wee, T.C. Sum, S.M. Tang, F. Watt, Sens. Actuators A 92 (2001) 370.
- [15] F. Schrempel, Y.-S. Kim, W. Witthuhn, Appl. Surf. Sci. 189 (2002) 102.
- [16] F. Watt et al., these Proceedings.
- [17] A.A. Bettioli, J.A. van Kan, T.C. Sum, F. Watt, Nucl. Instr. and Meth. B 181 (2001) 49.
- [18] E.H. Lee, G.R. Rao, L.K. Mansur, Radiat. Phys. Chem. 55 (1999) 293.